Multiparametric QUS Analysis for Placental Tissue Characterization

Farah Deeba, Manyou Ma, Mehran Pesteie, Jefferson Terry, Denise Pugash, Jennifer A. Hutcheon, Chantal Mayer, Septimiu Salcudean and Robert Rohling

Abstract— **Multiparametric Quantitative Ultrasound (QUS) holds promise for characterizing placental tissue and detecting placental disorders. In this study, we simultaneously extract two qualitatively different QUS parameters, namely attenuation coefficient estimate (ACE) and shear wave speed from ultrasound radio frequency data acquired using a shear wave vibro elastography (SWAVE) method. The study comprised data from 59 post-delivery clinically normal placentas. The shear wave speed was found to be equal to 1.74 ± 0.13 m/s whereas the attenuation coefficient estimate was 0.57 ± 0.48 dB/cm-MHz. This provides a baseline for future studies of placental disorders.**

I. Introduction

The placenta forms the critical interface between the fetus and the mother, and is responsible to provide a safe and protective milieu for fetal development. Placental dysfunction plays a central role in the development of pre-eclampsia, fetal growth restriction, and pre-term labor and may be responsible for a significant proportion of maternal and perinatal mortality and morbidity [1], [2]. Despite advances in perinatal care and extensive research efforts, there has not been substantial improvement in the prediction and prevention of these disorders [3], [4]. Due to the multi-etiologic nature of placental disorders, any single test is not adequate to identify all or most of the cases [1]. Therefore, the importance of developing an effective multiparametric screening system based on non-invasive techniques to improve early detection of placental disorder, cannot be overstressed.

Placental disorders involve both macro- and microstructural changes of the tissue. Quantitative ultrasound (QUS), with the ability to characterize tissue microstructure, is a suitable candidate for developing an effective screening tool. Among the QUS parameters, placental elasticity measured using elastography has exhibited initial promise in indicating placental diseases. Elastography is a non-invasive technique where an external force is applied to measure the mechanical properties of tissue, such as shear wave speed and Young's modulus. Significant increases in these elasticity measures have been found in patients with pre-eclampsia and IUGR [5]–[7]. Attenuation coefficient estimate (ACE) is another important QUS parameter, defined as the power dissipated per unit of propagation distance per unit frequency. In the field of obstetrics, attenuation has been exploited in predicting the risk of preterm labor by detecting cervical ripening from the ACE measured at cervix [9], but only preliminary work has been performed on placenta [10]. Based on the success of ACE in detecting fat contents [18] in liver and evidences showing high fat content in complicated pregnancy [19], we hypothesize that ACE could be a potential biomarker to detect complications in pregnancy.

In this paper, we explore the feasibility of characterizing placental tissue using both the shear wave speed and ACE, using radio frequency (RF) data collected from a shear wave vibro-elastography (SWAVE) study. Placenta specimens were subject to an external excitation that generated a shear wave within them and an ultrasound scanner was used to measure the shear wave speed. The ultrasound radio frequency (RF) data acquired while applying the mechanical excitation contained information from both the shear wave and the longitudinal wave. These two entities conveyed qualitatively different information due to differences in wavelength. Simultaneous measurement of elasticity and ACE parameters resulting from these two wave propagations would also meet the multi-parametric requirement to detect certain placental disorders. The objective of the study was to establish reliable baseline measurements with controlled variables, which is an important step for placental characterization *in-vivo*.

The main contributions of this work are as follows. To our knowledge, this is the first comprehensive study to report the baseline attenuation coefficient based on a large cohort of clinically normal placentas (n = 59). The work explores the feasibility of simultaneous computation of ACE and shear wave speed from the same ultrasound RF data. Furthermore, this study investigates the spatial correlation between ACE and shear wave speed, analyzes their values for different sub-classes, and tissues near maternal and fetal surface.

II. Methodology

A. Study Population

Full-term placentas (n=59) with gestational age between 37-41 weeks were collected after delivery from pregnant women aged 19 to 47 years. This study (H15-00974) was performed after approval by the University of British Columbia Children's and Women's Research Ethics Board, and written informed consent. After delivery, the placentas were immediately stored at 4° C for an average of 4 hours and warmed to 37° C by immersion in a constant temperature water bath to simulate the temperature *in vivo* before

*Research supported by the Natural Sciences and Engineering Research Council of Canada and the Canadian Institutes of Health Research.

F. Deeba, M. Ma, M. Pesteie, S. Salcudean and R. Rohling are with the Department of Electrical and Computer Engineering, University of British Columbia, Vancouver, British Columbia, Canada (e-mail: rohling@ece.ubc.ca).

J. Terry is with the Department of Pathology and Laboratory Medicine, C. Mayer and J. A. Hutcheon are with the Department of Obstetrics and Gynecology, and Dr. Pugash is with the Department of Radiology, all at the University of British Columbia, Vancouver, British Columbia, Canada.

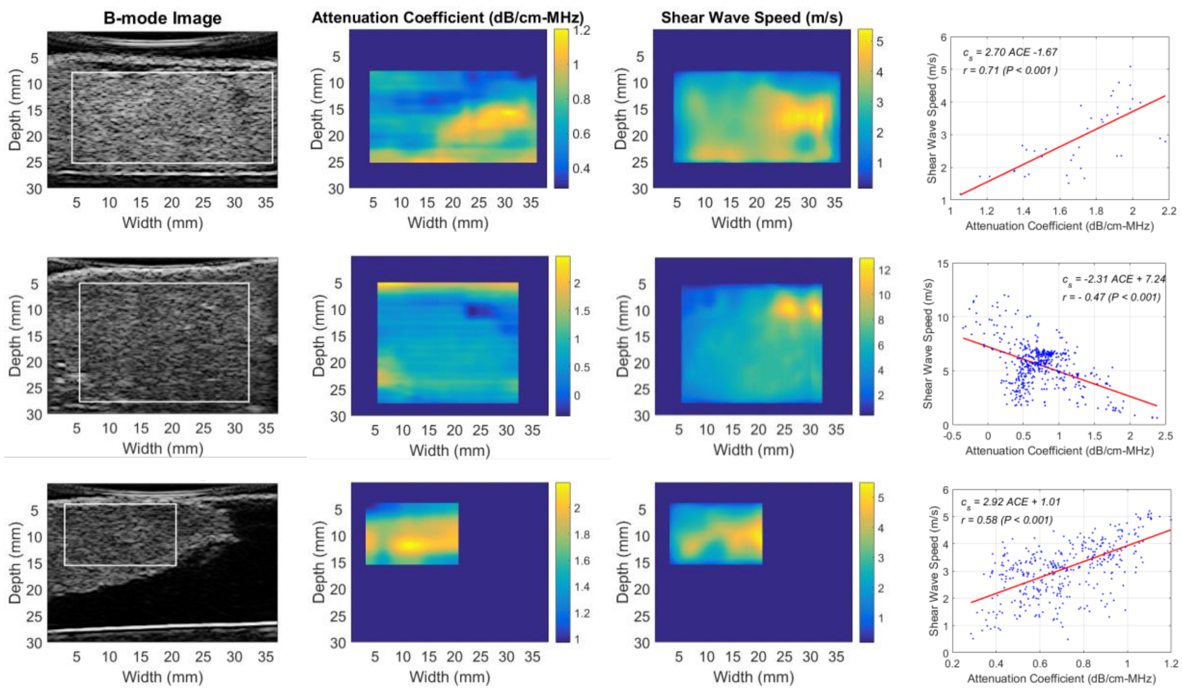

(a) (b) (c) (d)

Figure 1: Example images of attenuation coefficient map and shear wave speed map for three examples from sub-class A (top), sub-class B (middle), and sub-class C (bottom). (a) Ultrasound B-mode image with region of interest (highlighted in white) used for ACE and c_s measurement, (b) attenuation coefficient map, (c) shear wave speed map, and (d) correlation between attenuation coefficient and shear wave speed, where r is the Pearson's correlation coefficient and P indicates the p-value. The attenuation coefficient map has been interpolated to provide resolution similar to the shear wave speed.

acquiring the RF data [11]. In this study, placentas were selected based on normal clinical features during pregnancy and confirmed by pathological examination after delivery. The placentas in this study were sub-divided into three categories. Sub-class A included 13 placentas without any specific macro- or microscopic lesions, sub-class B includes 30 placentas manifesting specific lesions that did not reach relevant diagnostic threshold, and sub-class C was comprised of 16 placentas with abnormalities passing one or more diagnostic thresholds [17]. It should be emphasized that regardless of the presence of the lesions, all the placentas were considered to be clinically normal based on the criteria that the pregnancies had no clinical complications. Therefore, the sub-classes encompass the different range of pathological spectrum occurred in clinically normal placentas.

B. *Experimental Setup*

The ultrasound RF data from *ex-vivo* placentas as well as the reference phantom used for computing ACE were acquired with a modular ultrasound system, comprising an Ultrasonix SonixTouch scanner (Analogic, Richmond, BC, Canada), using a 4DL14-5/38 4D linear transducer operated at 5 MHz transmit frequency. A voice coil exciter (LDS V203, Brüel & Kjær, Nærum, Denmark) was used to apply excitation onto the placenta surface. The ultrasound system was equipped with the Porta research interface that facilitated the development of SWAVE, an elastography system in our lab [12]. The time-gain compensation (TGC) curve, power level, depth, and focus were adjusted to maximize image quality. Accordingly, the depth was set to 3 cm with a focus at 2 cm to capture the full thickness of full-term placentas. The system collected volumetric RF data at 10 positions, with an angle increment of 0.4°. An ultrasound volume was collected at five excitation frequencies: 60, 80, 90, 100 and 120 Hz. The same system settings were used to acquire ultrasound RF data from a multipurpose multi-tissue ultrasound phantom (model 040GSE, CIRS, Norfolk, VA), for normalizing the placenta power spectrum as required in attenuation coefficient estimation with the reference phantom method. The phantom has two separated attenuation regions with attenuation coefficients 0.5 dB/cm-MHz and 0.7 dB/cm-MHz and speed of sound 1540 m/s as reported by the manufacturer.

C. *Shear Wave Speed Estimation*

Cross-correlation and cosine interpolation [20] was used to compute the shear wave motion along the axial direction of the transducer. Then, the shear wave speed was computed from the scan converted shear wave motion phasors using a set of log-normal quadrature filters [13]. The resulting shear wave speed c_s at a frequency ω can be expressed as:

$$c_s = \frac{\omega}{k}, \quad (1)$$

where k is a weighted sum of the values obtained from the directional filters. Shear wave speed was measured from a manually selected region-of-interest (ROI), the criteria of which was to be the maximum rectangular area limited within the placenta. In the subsequent calculations, we used the mean shear wave speed obtained after averaging shear wave speed values for five different excitation frequencies.

A. *Attenuation Coefficient Estimation*

The ACE was measured using the reference phantom method [14]. According to this method, the attenuation of the

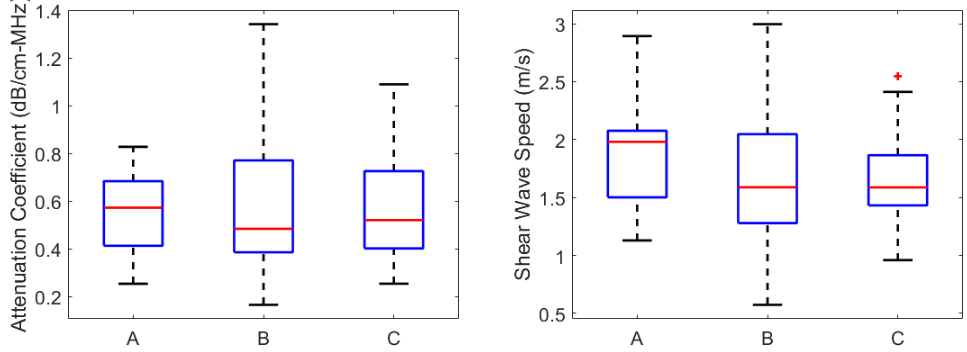

(a) (b)

Figure 2: Box and whisker plots of (a) attenuation coefficient, (b) shear wave speed for three sub-classes of placentas. The boxes represent the first and third quartiles, whiskers represent the range, and lines in the box represent the median values of the distribution. The (+) symbols represent the outliers.

placenta, α_s at each frequency component can be calculated from the slope of the straight line that fits the following equation:

$$\alpha_s(f) = \alpha_r(f) - \frac{1}{4}\frac{\partial\big(RS(f,z)\big)}{\partial z}, \tag{2}$$

where $RS(f,z)$ is the ratio of the power spectrum from the placenta sample to the reference phantom at frequency f for a time-gated RF signal window centered at depth z, and α_r is the corresponding attenuation in the reference material. Assuming a linear frequency dependence, the ACE, β_s of a placenta sample can be estimated by measuring the slope of the straight line that fits the following equation:

$$\alpha_s(f) = f.\beta_s(f). \tag{3}$$

The ACE values were measured in the same ROI selected for c_s computation. The dimension of each time-gated window for computing power spectra was selected to be $N = 30$ scanlines (8 uncorrelated scanlines) laterally and $\Delta z = 7.7$ mm (400 samples or 24 pulse lengths) axially. Axially, five time-gated windows were used as regression points to measure ACE, β_s. The attenuation estimation regions were spaced at one pulse-echo correlation length, both axially and laterally [15].

III. Results

We generated the attention coefficient estimate (ACE) map and the shear wave speed (c_s) map in the same ROI for all 59 placenta samples. Examples of images are shown in Fig. 1. We observed cases where the ACE map and c_s map show a similar pattern indicating a common influence by the underlying structure. The c_s and ACE values appeared to be spatially correlated, as is evident from Figure 1(d). However, the correlation pattern varied for different cases. We hypothesize that the underlying structure of the placenta is heterogeneous, so we expect different correlation patterns between ACE and c_s for different underlying structure. Moreover, the weak correlation indicates that the ACE and c_s provide complementary, and therefore non-redundant structural information. This also agrees to the previous study on liver attenuation and elasticity where a mild but significant correlation was found between these two parameters ($P = 0.013$) [16]. The interdependency of ACE and c_s measurements for placenta will be explored in the future.

We measure the ACE and c_s values for the three sub-classes as described in section II-A. Fig. 2 shows the box and whisker representations of ACE and c_s for the three sub-classes. We performed a Kruskal-Wallis test to determine whether a statistically significant difference existed among the three sub-classes. The differences among the three sub-classes did not reach statistical significance ($p = 0.55$). Similarly, the c_s measures for the three sub-classes were not significantly different ($p = 0.34$). The result was expected as the placentas in all three sub-classes belong to clinically normal class. We report the mean and average standard deviation (intra-subject) for all three sub-classes and for all data in Table I. The shear wave speed was found to be equal to 1.74 ± 0.13 m/s whereas the ACE was 0.57 ± 0.48 dB/cm-MHz, obtained using the entire dataset. A prior study reported ACE within a range of $0.76 - 0.85$ dB/cm-MHz at 36-40 weeks for n=4 population size [10]. The ACE value reported by our study is within reasonable agreement with the previous study. The c_s values are also consistent with the previous studies [11]. The effect of perfusion was not included here. However, a previous study found mean c_s value equal to 1.92 ± 0.05 m/s in an open perfusion system [21], which is similar to the values obtained without perfusion. But the effect of perfusion on ACE is still to be explored. In order to compute the mean and standard deviation of c_s, a smaller ROI was used to optimize the quality of elasticity measurements, which was same as to the previous study [11]. However, no such selection was made for ACE computation. Nevertheless, the high estimation variation of ACE measures emphasizes the importance of selecting optimal ROI for ACE computation.

In addition, we compared the ACE and c_s values from regions near the maternal surface and the fetal surface. We performed a Mann-Whitney U test between these two classes.

Table 1: Shear wave speed and attenuation coefficient for placenta samples (n=59).

Sub-classes	ACE (dB/cm-MHz)		Shear Wave Speed (m/s)	
	Mean	Std. Dev.	Mean	Std. Dev.
A	0.54	0.41	1.91	0.12
B	0.58	0.49	1.72	0.13
C	0.60	0.50	1.66	0.16
All Placentas	0.57	0.48	1.74	0.13

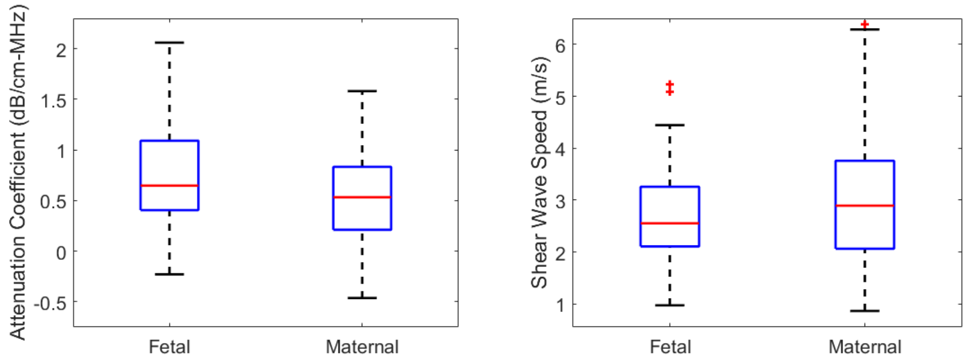

(a) (b)

Figure 3: Box and whisker representation of (a) attenuation coefficient, and (b) shear wave speed for region-of-interest near the fetal surface and near the maternal surface. The boxes represent the first and third quartiles, whiskers represent the range, and lines in the box represent the median values of the distribution. The (+) symbols represent the outliers.

The box and whisker plot is provided in Figure 3. We found that the fetal side is associated with higher attenuation coefficient compared to the maternal side (p = 0.03). This could be a consequence of the relatively larger (stem) villi present at the fetal side. However, the difference in shear wave speed values between the maternal side and fetal side was not found to be statistically significant.

IV. Conclusion

This study shows the application of the ultrasound data for simultaneous multiparametric measurement, namely attenuation coefficient estimate and shear wave speed for placental tissue characterization. The placenta has received relatively little attention in the QUS literature compared with other organs, and this work presents the first large-scale study to report the baseline values for ACE and shear wave speed based on the examination of 59 clinically normal full-term placentas. Investigation into classes and spatial variations suggests exciting avenues for future research. The weak spatial correlation observed between these ACE and shear wave speed could play a complimentary role in identifying clinically significant abnormalities. In future work, we will extend the study to compare attenuation coefficient estimate and shear wave speed between normal and diseased placentas.

Acknowledgments

We wish to thank Caitlin Schneider, Mohammad Honarvar and Julio Lobo for help with the implementation.

References

[1] R. Romero, "Prenatal medicine: The child is the father of the man," *J. Matern. Neonatal Med.*, vol. 22(8), pp. 636-639, 2009.

[2] T. K. Morgan, "Role of the Placenta in Preterm Birth: A Review," *Am. J. Perinatol.,* vol. 33(3), pp. 258266, 2016.

[3] O. M. Faye-Petersen, "The placenta in preterm birth," *J. Clin. Pathol.*, vol. 61(12), pp. 1261-1275, 2008.

[4] Baha Sabai, Gus Dekker, and Michael Kupferminc, "Pre-eclampsia," *Lancet*, vol. 365(9641), pp. 785-99, 2005.

[5] G. Durhan, et al. "Placental elasticity and histopathological findings in normal and intra-uterine growth restriction pregnancies assessed with strain elastography in ex vivo placenta," *Ultrasound in Medicine and Biology*, vol. 43(1), pp. 111–8, Jan 2017.

[6] M. Sugitani, et al. "A new method for measurement of placental elasticity: acoustic radiation force impulse imaging." *Placenta*, vol. 34(11), pp. 100–1013, 2013.

[7] C. Cimsit, T. Yoldemir, and I. N. Akpinar, "Strain elastography in placental dysfunction: placental elasticity differences in normal and preeclamptic pregnancies in the second trimester," *Archives of gynecology and obstetrics*, vol. 291(4), pp. 811–817, 2015.

[8] Michael L. Oelze, and J. Mamou, "Review of quantitative ultrasound: Envelope statistics and backscatter coefficient imaging and contributions to diagnostic ultrasound*," IEEE trans. on Ultrasonics, Ferroelectrics, and Frequency Control*, vol. 63(2), pp. 336–35, 2016.

[9] L. Yassin, T. A. Bigelow, B. L. McFarlin, "Estimate of the attenuation coefficient using a clinical array transducer for the detection of cervical ripening in human pregnancy," *Ultrasonics*, vol. 51 (1), pp. 34–39, 2011.

[10] J. Caloone, et al. "High-intensity focused ultrasound applied to the placenta using a toroidal transducer: A preliminary ex-vivo study," *Ultrasound Obstet. Gynecol.* vol. 45 (3), pp. 313–319, 2015.

[11] J. M. Abeysekera, et al. "SWAVE Imaging of Placental Elasticity and Viscosity: Proof of Concept," *Ultrasound Med. Biol.* 43 (6), pp. 1112-1124, 2017.

[12] J. M. Abeysekera, "Three Dimensional ultrasound imaging," Ph.D. thesis, 2016.

[13] H. Knutsson, C-F. Westin, and G. Granlund, "Local multiscale frequency and bandwidth estimation," *In Image Processing, 1994. Proceedings. ICIP-94., IEEE Int. Conf.*, vol. 1, IEEE, 1994.

[14] L. X. Yao, J. A. Zagzebski, E. L. Madsen, "Backscatter coefficient measurements using a reference phantom to extract depth-dependent instrumentation factors," *Ultrason. Imaging*, vol. 12 (1), pp. 58-70, 1990.

[15] I. M. Rosado-Mendez, et al. "Task-Oriented Comparison of Power Spectral Density Estimation Methods for Quantifying Acoustic Attenuation in Diagnostic Ultrasound Using a Reference Phantom Method," *Ultrasonic imaging,* vol. 35 (3), pp. 320-331, 2013.

[16] J. M. Ahn, et al. "Relationship of liver stiffness and controlled attenuation parameter measured by transient elastography with diabetes mellitus in patients with chronic liver disease." *Jour. of Kor. Med. Scie.,* vol. 29.8, pp. 1113-1119, 2014.

[17] T. Y. Khong, et al. "Sampling and definitions of placental lesions: Amsterdam placental workshop group consensus statement," *Archives of pathology & laboratory medicine,* vol. 140.7, pp. 698-713, 2016.

[18] Y. Kanayama, et al. "Real-time ultrasound attenuation imaging of diffuse fatty liver disease," *Ultrasound Med. Biol.*, vol. 39.4, pp. 692-705, 2013.

[19] S. H. Brown, et al. "A lipidomic analysis of placenta in preeclampsia: Evidence for lipid storage," *PLoS One*, vol. 11.9, pp. 1-13, 2016.

[20] I. Céspedes, et al. "Methods for estimation of subsample time delays of digitized echo signals", *Ultrasonic Imaging*, vol. 17, no. 2, pp. 142–171, 1995.

[21] S. A. McAleavey, et al. "Shear wave elastography in the living, perfused, post-delivery placenta." *Ultrasound in Med. & Biol., vol.*, 42.6, pp. 1282-1288, 2016.